

Quantum-jump vs stochastic Schrödinger dynamics for Gaussian states with quadratic Hamiltonians and linear Lindbladians

Robson Christie, Jessica Eastman and Eva-Maria Graefe

Department of Mathematics, Imperial College London, London SW7 2AZ, United Kingdom

E-mail: robson.christie13@imperial.ac.uk, j.eastman@imperial.ac.uk and e.m.graefe@imperial.ac.uk

23 March 2022

Abstract. The dynamics of Gaussian states for open quantum systems described by Lindblad equations can be solved analytically for systems with quadratic Hamiltonians and linear Lindbladians, showing the familiar phenomena of dissipation and decoherence. It is well known that the Lindblad dynamics can be expressed as an ensemble average over stochastic pure-state dynamics, which can be interpreted as individual experimental implementations, where the form of the stochastic dynamics depends on the measurement setup. Here we consider quantum-jump and stochastic Schrödinger dynamics for initially Gaussian states. While both unravellings converge to the same Lindblad dynamics when averaged, the individual dynamics can differ qualitatively. For the stochastic Schrödinger equation, Gaussian states remain Gaussian during the evolution, with stochastic differential equations governing the evolution of the phase-space centre and a deterministic evolution of the covariance matrix. In contrast to this, individual pure-state dynamics arising from the quantum-jump evolution do not remain Gaussian in general. Applying results developed in the non-Hermitian context for Hagedorn wavepackets, we formulate a method to generate quantum-jump trajectories that is described entirely in terms of the evolution of an underlying Gaussian state. To illustrate the behaviours of the different unravellings in comparison to the Lindblad dynamics, we consider two examples in detail, which can be largely treated analytically, a harmonic oscillator subject to position measurement and a damped harmonic oscillator. In both cases we highlight the differences as well as the similarities of the stochastic Schrödinger and the quantum-jump dynamics.

1. Introduction

A large class of open quantum systems can be described by Lindblad equations for the dynamics of density operators. In many atomic physics and quantum optics applications, this is an accurate description of physical phenomena. Lindblad dynamics can be viewed as an ensemble average over stochastic pure-state trajectories. The stochastic trajectories may be interpreted as the state of an individual experimental quantum

system conditioned on a measurement record. The nature of the measurement record determines the types of trajectories in the ensemble [1, 2, 3], and intriguingly can lead to strikingly different microscopic dynamics and behaviours, while averaging to the same Lindblad dynamics. An example of this has been reported in [4] where it has been demonstrated that depending on the specific unravelling a dissipative Kerr dynamics can lead to switches between either odd and even Schrödinger cat states or between coherent states of opposite phase. It has been observed in examples that individual stochastic trajectories can even display chaotic dynamics that are not seen in the ensemble average [5].

Two of the most important unravellings are given by *stochastic Schrödinger equations* (SSEs) and *quantum-jump* trajectories, respectively. The SSE dynamics is a good description of certain homodyne and heterodyne detection schemes in quantum optics arising from constant weak continuous measurements [6]. Quantum-jump dynamics, on the other hand, may arise in photodetection experiments and is theoretically described by periods of deterministic evolution under an effective non-Hermitian Hamiltonian, stochastically interrupted by discrete measurements [7]. In both SSE and quantum-jump scenarios, if the measurement channel is not recorded, then the best estimate for the state is obtained by averaging over all possibilities, resulting in Lindblad dynamics [6]. There are other interpretations of the unravellings of the Lindblad equation, viewing them as candidate laws of nature in an effort to explain the wavefunction collapse in quantum measurement (see e.g. [8, 9, 10, 11] for more details).

In the present paper, we analyse in detail the structural differences of these unravellings as compared to the full Lindblad dynamics for the case of quadratic Hamiltonians and linear Lindbladians for initial Gaussian states. In these cases the full quantum dynamics in the Lindblad case can be reduced to simple phase-space dynamics, as has been discussed in [12, 13]. This follows the spirit of Heller's and Littlejohn's approach to closed system dynamics [14, 15] where for a quadratic Hamiltonian initially Gaussian states remain Gaussian under time evolution. This idea carries through to the SSE [16, 17]. Since Gaussian states may be parameterised entirely by their centres and covariances, the dynamics of these systems may be transformed from state vector dynamics in infinite-dimensional Hilbert space to a handful of differential equations for classical phase-space observables. This simple approach does not carry through to the quantum-jump dynamics, which in general do not preserve Gaussian states for arbitrary linear Lindbladians. Here we present a different approach that builds on an extension of Hagedorn's wavepacket dynamics [18] that has been adapted to non-Hermitian systems in [19].

In detail, the paper is organised as follows. In section 2 we introduce the Lindblad equation along with the quantum-jump and SSE unravellings. In section 3 we insert an initially Gaussian state into the SSE and derive a set of stochastic differential equations which is exact in the case of quadratic Hamiltonians and linear Lindbladians. The resulting parameter dynamics are less computationally expensive to simulate than the full state vector dynamics. In section 4 we briefly review the non-Hermitian dynamics

of Gaussian states and then apply the non-Hermitian Hagedorn wavepacket dynamics developed in [19] to formulate a semi-analytical algorithm for simulating quantum-jump trajectories. In section 5 we illustrate our findings for two examples which we consider in some detail: A harmonic oscillator Hamiltonian with either a position measurement, modelled by a Lindbladian $\hat{L} = \hat{x}$, or a radiative decay, modelled by a Lindbladian $\hat{L} = \hat{a}$. We conclude with a short summary and outlook in section 6.

2. Unravellings of the Lindblad Equation

The Lindblad equation was initially derived as the most general Markovian dynamical equation that preserves the trace, Hermiticity and positivity of the density matrix [20, 21]. Physically, it can be used to describe certain quantum systems that are weakly coupled to a memoryless environment. In this spirit, dynamics of Lindblad form can be obtained for the reduced density matrix by averaging over the effect of a bath of quantum harmonic oscillators [22]. Any linear and Markovian (local in time) master equation that preserves the Hermiticity and trace of the density matrix may be expressed in Lindblad form,

$$i\hbar \frac{d}{dt} \hat{\rho}(t) = [\hat{H}, \hat{\rho}(t)] + i \sum_k [\hat{L}_k \hat{\rho}(t) \hat{L}_k^\dagger - \frac{1}{2} \hat{L}_k^\dagger \hat{L}_k \hat{\rho}(t) - \frac{1}{2} \hat{\rho}(t) \hat{L}_k^\dagger \hat{L}_k]. \quad (1)$$

Here \hat{H} is a Hamiltonian and \hat{L}_k are general Lindblad operators, the properties of which are system-specific. For simplicity in what follows we shall confine the discussion to a single Lindblad operator.

Much like the deterministic Fokker-Planck equation for the dynamics of probability distributions in classical physics admits *unravellings* in terms of single trajectories of the stochastic Langevin equation, the deterministic Lindblad equation for the dynamics of the density operator may be unravelled in terms of stochastic pure-state trajectories. There are infinitely many such unravellings that differ from each other in the stochastic driving processes. The two types of unravellings most commonly considered in the literature are SSE trajectories [11] driven with continuous Gaussian distributed noise, and quantum-jump [7] trajectories driven by discrete Poissonian distributed noise.

The SSE we consider here is given by [11, 16]

$$\begin{aligned} |d\psi\rangle &= \frac{1}{\hbar} \left(-i\hat{H} - \frac{1}{2} \hat{L}^\dagger \hat{L} + \langle \hat{L}^\dagger \rangle_\psi \hat{L} - \frac{1}{2} \langle \hat{L}^\dagger \rangle_\psi \langle \hat{L} \rangle_\psi \right) |\psi\rangle dt \\ &\quad + \frac{1}{\sqrt{2\hbar}} (\hat{L} - \langle \hat{L} \rangle_\psi) |\psi\rangle (d\xi_R + id\xi_I), \end{aligned} \quad (2)$$

where $d\xi_R$ and $d\xi_I$ are independent ($\mathbb{E}[d\xi_R d\xi_I] = 0$) Itô stochastic processes with mean zero ($\mathbb{E}[d\xi_R] = \mathbb{E}[d\xi_I] = 0$) and normalisation $d\xi_R^2 = d\xi_I^2 = dt$. The SSE trajectories are driven with a continuous stochastic process and are often used to model systems undergoing weak continuous measurement such as heterodyne detection in quantum optics [6] or quantum Brownian motion [22].

In the quantum-jump description, on the other hand, the pure-state trajectories deterministically evolve under an effective non-Hermitian Hamiltonian $\hat{H} - i\hat{\Gamma}$ with $\hat{\Gamma} = \frac{1}{2}\hat{L}^\dagger\hat{L}$, periodically interrupted by stochastic quantum jumps. These jumps may be used to represent random discrete measurements of quantum systems such as photodetection from a microwave cavity [6]. The cumulative effect of these jumps when averaged over many trajectories induce the “jump term” contribution $\hat{L}\hat{\rho}(t)\hat{L}^\dagger$ in the density operator dynamics. Concretely, quantum-jump pure-state dynamics can be described by the dynamical equation

$$\begin{aligned} |d\psi\rangle = & \frac{1}{\hbar} \left(-i\hat{H} - \frac{1}{2}\hat{L}^\dagger\hat{L} - \frac{1}{2}\langle\hat{L}^\dagger\hat{L}\rangle_\psi \right) |\psi\rangle (1 - dN) dt \\ & + \left(\frac{\hat{L}}{\langle\hat{L}^\dagger\hat{L}\rangle_\psi} - 1 \right) |\psi\rangle dN. \end{aligned} \quad (3)$$

Here dN is a Poisson process, taking the values 0 (no jump) or 1 (jump) with expectation value $\mathbb{E}[dN] = \langle\hat{L}^\dagger\hat{L}\rangle_\psi dt$. The following algorithm [1] is equivalent to eq. (3):

- (i) Discretise the time interval $(t_0, t_N) \rightarrow \{t_k\}$ with $\Delta t = t_{k+1} - t_k$;
- (ii) Pick a random number R from the uniform distribution on the interval $[0, 1]$;
- (iii) For all t_k with $t_0 < t_k \leq t_N$ evaluate the following loop:

```

for k=1:N-1
    if R ≥ ||ψ_k||^2 % Jump
        |ψ_{k+1}\rangle = Ā |ψ_k\rangle / ⟨Ā^\daggerĀ⟩
        R=rand~U(0, 1)
    else % No jump
        |ψ_{k+1}\rangle = |ψ_k\rangle - Ā(Ā - Ā^\daggerĀ) |ψ_k\rangle Δt
    end
end

```

- (iv) Normalise the entire trajectory; $|\psi_k\rangle \rightarrow |\psi_k\rangle / ||\psi_k||$ for all k .

Considering quantum-jump trajectories of a Markovian open system described by the Lindblad master equation and postselecting only trajectories in which no jumps have occurred, thus leads to effective non-Hermitian Hamiltonian dynamics [23, 24, 25]. Quantum dynamics generated by non-Hermitian Hamiltonians is an active area of research on its own, and we will make use of some techniques developed in this context [26, 19]. It should be noted that $\hat{L}^\dagger\hat{L}$ is a positive operator and thus non-Hermitian Hamiltonians, $\hat{H} - \frac{i}{2}\hat{L}^\dagger\hat{L}$, arising in the context of postselection of Lindblad/quantum-jump dynamics may only describe loss (but not gain).

Despite converging to the same ensemble dynamics, the SSE and quantum-jump trajectories can differ not just quantitatively but qualitatively. We will analyse these differences in detail for quadratic Hamiltonians and linear Lindblads with initially Gaussian states. While for Lindblad and SSE dynamics the Wigner function remains

Gaussian for all times for quadratic Hamiltonians and linear Lindbladians, this is in general not the case for quantum-jump dynamics, even though averaging over quantum-jump trajectories recovers the Gaussian Lindblad results. We will return to this issue after considering the Gaussian Lindblad and SSE dynamics.

3. Gaussian dynamics

Gaussian states are well suited for the analysis of quantum dynamics, since they are localised in phase space on order \hbar (in appropriate coordinates they are minimum uncertainty states), and are the only states with a completely positive Wigner function [27]. In this regard they may be thought of as the most “classical” of quantum states [28], and Gaussian approximations of the full quantum dynamics lead to simple phase-space dynamics. As has been observed by Schrödinger already in the early days of quantum mechanics, Gaussian wavepackets remain Gaussian in the dynamics of quantum harmonic oscillators and follow classical trajectories. For open systems described by Lindblad equations or Schrödinger dynamics generated by non-Hermitian Hamiltonians, a similar statement holds, which allows to reduce the full quantum Hilbert space dynamics to a simple phase-space dynamics described by a handful of parameters for Gaussian states for quadratic Hamiltonians and linear Lindbladians [26, 29, 13]. Gaussian evolution for stochastic Schrödinger equations with quadratic Hamiltonian and linear Lindbladians in position representation has been considered in [17, 30, 31], and here too, an initial Gaussian state remains Gaussian.

In what follows we shall provide a brief review of the derivation and result for Lindblad dynamics, and then extend the idea to stochastic Schrödinger dynamics in quantum phase space, where we use the Wigner-Weyl formalism that illuminates the underlying phase-space geometry and allows for a better direct comparison with the Lindblad dynamics. We will consider Gaussian Wigner functions of the form

$$W(z) = \frac{\sqrt{\det G}}{\pi\hbar} e^{-\frac{1}{\hbar}\delta z \cdot G \delta z} \quad \text{with} \quad \delta z = \begin{pmatrix} x - \langle x \rangle \\ p - \langle p \rangle \end{pmatrix} = z - \tilde{z}, \quad (4)$$

with a real symmetric matrix G , that encodes the phase-space covariance matrix of the system as

$$\Sigma_{ij} = \Delta(z_i z_j)^2 = \frac{\hbar}{2} G_{ij}^{-1}. \quad (5)$$

This describes a pure state if and only if $\det G = 1$ [32]. Inserting an ansatz of the form (4) with time-dependent (and in the SSE case stochastic) parameters G and \tilde{z} into the evolution equation for the Wigner function yields dynamical equations for the parameters.

3.1. Gaussian dynamics of the Lindblad equation

The Lindblad equation in Weyl representation takes the form

$$\frac{dW}{dt} = \frac{1}{\hbar} \left(-i(H \star W - W \star H) + L \star W \star \bar{L} - \frac{1}{2} \bar{L} \star L \star W - \frac{1}{2} W \star \bar{L} \star L \right), \quad (6)$$

with the Moyal (star) product of Weyl symbols given by

$$(A \star B)(q, p) = A(q, p) e^{\frac{i\hbar}{2} \vec{\nabla} \cdot \Omega \cdot \vec{\nabla}} B(q, p). \quad (7)$$

Since we are considering only quadratic Hamiltonians and linear Lindbladians, the Moyal products in eq. (6) can be fully expanded to yield [13]

$$\frac{dW}{dt} = -i\nabla \bar{L} \cdot \Omega \nabla L W + \nabla H \cdot \Omega \nabla W + \text{Im}(L \nabla \bar{L}) \cdot \Omega \nabla W - \frac{\hbar}{2} \text{Re}(\nabla L \cdot \Omega W'' \Omega \nabla \bar{L}), \quad (8)$$

where

$$\Omega = \begin{pmatrix} 0 & 1 \\ -1 & 0 \end{pmatrix} \quad (9)$$

is the symplectic matrix. An initial Gaussian state remains Gaussian for all times [13]. It is useful to rewrite H and L as polynomials in δz

$$\begin{aligned} H(z) &= H(\tilde{z}) + \nabla H|_{z=\tilde{z}} \cdot \delta z + \frac{1}{2} \delta z \cdot H''|_{z=\tilde{z}} \delta z \\ L(z) &= L(\tilde{z}) + \nabla L|_{z=\tilde{z}} \cdot \delta z, \end{aligned} \quad (10)$$

where we have used a Taylor series (which is exact here) to identify the linear and quadratic coefficients. We substitute these expansions into eq. (8) to obtain

$$\begin{aligned} \frac{dW}{dt} &= \left[-\frac{2}{\hbar} (\nabla H + H'' \delta z) \cdot \Omega G \delta z - \frac{2}{\hbar} \text{Im}(L \nabla \bar{L}) \cdot \Omega G \delta z - \frac{2}{\hbar} \text{Im}(\nabla L \nabla \bar{L}) \cdot \Omega G \delta z \right. \\ &\quad \left. - i\nabla \bar{L} \cdot \Omega \nabla L + \text{Re}(\nabla L \cdot \Omega G \Omega \nabla \bar{L}) - \frac{2}{\hbar} \delta z \cdot G \Omega \text{Re}(\nabla L \nabla \bar{L}^T) \Omega G \delta z \right] W. \end{aligned} \quad (11)$$

On the other hand, taking the time derivative of eq. (4) we find

$$\frac{dW}{dt} = \left(\frac{1}{2} \text{Tr}(G^{-1} \dot{G}) + \frac{2}{\hbar} \dot{\tilde{z}} \cdot G \delta z - \frac{1}{\hbar} \delta z \cdot \dot{G} \delta z \right) W. \quad (12)$$

Comparing coefficients of δz in (11) and (12) we obtain the dynamical equations

$$\begin{aligned} \frac{d\tilde{z}}{dt} &= \Omega \nabla H + \Omega \text{Im}(L \nabla \bar{L}) \\ \frac{dG}{dt} &= (H'' + \text{Im}(\nabla L \nabla \bar{L}^T)) \Omega G - G \Omega (H'' - \text{Im}(\nabla L \nabla \bar{L}^T)) \\ &\quad + 2G \Omega \text{Re}(\nabla L \nabla \bar{L}^T) \Omega G \end{aligned} \quad (13)$$

for the dynamics of the Gaussian parameters. The first order differential equation describing the central motion is linear and can be trivially integrated. The dynamical

equation for the covariance matrix G decouples from the central motion as the Hamiltonian and Lindbladian dependent terms become constant. The general solution can be obtained as (see [33] and references therein)

$$G(t) = [2D(t) + (R^T(-t)G^{-1}(0)R(-t))^{-1}]^{-1}, \quad (14)$$

where

$$R(t) = e^{(\Omega H'' + \text{Im}(\nabla L \nabla \bar{L}^T) \Omega)t} \quad (15)$$

and

$$D(t) = \int_0^t R(s) \text{Re}(\nabla L \nabla \bar{L}^T) R^T(s) ds. \quad (16)$$

For Hermitian Lindbladians, the Lindblad term in the central dynamics vanishes leaving only Hamiltonian dynamics, as expected for these *purely decohering* systems. In general non-Hermitian Lindbladians lead to both decoherence (that may be characterised by the evolution of G in our case) and dissipation that leads to non-Hamiltonian dynamics of the centre of the Gaussian.

3.2. Gaussian Stochastic Schrödinger dynamics

Let us now use the same approach to derive parameter dynamics for the SSE. We begin by writing the SSE in projector form as

$$\begin{aligned} d(|\psi\rangle\langle\psi|) &= |d\psi\rangle\langle\psi| + |\psi\rangle\langle d\psi| + |d\psi\rangle\langle d\psi| \\ &= \frac{1}{\hbar}(-i\hat{H} - \frac{1}{2}\hat{L}^\dagger\hat{L} + \langle\hat{L}^\dagger\rangle_\psi\hat{L} - \frac{1}{2}\langle\hat{L}^\dagger\rangle_\psi\langle\hat{L}\rangle_\psi) |\psi\rangle\langle\psi| dt \\ &\quad + \frac{1}{\sqrt{2\hbar}}(\hat{L}\hat{\rho} + \hat{\rho}\hat{L}^\dagger - \langle\hat{L} + \hat{L}^\dagger\rangle\hat{\rho})d\xi_R + \frac{i}{\sqrt{2\hbar}}(\hat{L}\hat{\rho} - \hat{\rho}\hat{L}^\dagger - \langle\hat{L} - \hat{L}^\dagger\rangle\hat{\rho})d\xi_I. \end{aligned} \quad (17)$$

The deterministic (dt) part of equation (17) is the same as that of the Lindblad eq. (8) which can evolve pure states into mixed states. In the SSE case, however, the state remains pure for all times, since the stochastic terms conspire to conserve the purity of the state.

We translate eq. (17) into the Wigner-Weyl representation to obtain

$$\begin{aligned} dW &= -\frac{i}{\hbar}[H \star W - W \star H + i(L \star W \star \bar{L} - \frac{1}{2}\bar{L} \star L \star W - \frac{1}{2}W \star \bar{L} \star L)]dt \\ &\quad + \frac{1}{\sqrt{2\hbar}}[L \star W + W \star \bar{L} - \langle\hat{L} + \hat{L}^\dagger\rangle W]d\xi_R + \frac{i}{\sqrt{2\hbar}}[L \star W - W \star \bar{L} - \langle\hat{L} - \hat{L}^\dagger\rangle W]d\xi_I. \end{aligned} \quad (18)$$

Since the deterministic part is the same as that of the Lindblad system eq. (8), we need only calculate the stochastic terms. We have

$$\frac{1}{\sqrt{2\hbar}}(L \star W + W \star \bar{L} - \langle\hat{L} + \hat{L}^\dagger\rangle W) = \sqrt{\frac{2}{\hbar}}(L^R - \langle L^R \rangle)W + \sqrt{\frac{\hbar}{2}}\{W, L^I\}, \quad (19)$$

and

$$\frac{i}{\sqrt{2\hbar}}(L \star W - W \star \bar{L} - \langle\hat{L} - \hat{L}^\dagger\rangle W) = -\sqrt{\frac{2}{\hbar}}(L^I - \langle L^I \rangle) + \sqrt{\frac{\hbar}{2}}\{W, L^R\}, \quad (20)$$

where $\{, \}$ denotes the Poisson bracket and L^R/L^I denote the real/imaginary parts of L . Using the expressions (19) and (20) equation (18) becomes

$$dW = [\{H, W\} + \text{Im}(L\{\bar{L}, W\}) - i\{\bar{L}, L\}W + \frac{\hbar}{2}\text{Re}\{L, \{\bar{L}, W\}\}]dt + (\sqrt{\frac{2}{\hbar}}(L^R - \langle L^R \rangle)W + \sqrt{\frac{\hbar}{2}}\{W, L^I\})d\xi_R - (\sqrt{\frac{2}{\hbar}}(L^I - \langle L^I \rangle) - \sqrt{\frac{\hbar}{2}}\{W, L^R\})d\xi_I. \quad (21)$$

As in the Lindblad case in section 3.1 we replace the Weyl symbols with their finite Taylor series eq. (10). Using

$$\begin{aligned} \sqrt{\frac{2}{\hbar}}(L^R - \langle L^R \rangle)W + \sqrt{\frac{\hbar}{2}}\{W, L^I\} &= \sqrt{\frac{2}{\hbar}}(\nabla L^R \cdot \delta z + \nabla L^I \cdot \Omega G \delta z)W, \\ -\sqrt{\frac{2}{\hbar}}(L^I - \langle L^I \rangle) + \sqrt{\frac{\hbar}{2}}\{W, L^R\} &= -\sqrt{\frac{2}{\hbar}}(\nabla L^I \cdot \delta z - \nabla L^R \cdot \Omega G \delta z)W, \end{aligned} \quad (22)$$

we find

$$\begin{aligned} dW = & \left[\frac{2}{\hbar} (\delta z \cdot G \Omega (H'' + \text{Im}(\nabla \bar{L} \nabla L^T)) \delta z - \delta z \cdot G \Omega \text{Re}(\nabla \bar{L} \nabla L^T) \Omega G \delta z \right. \\ & - (\nabla H + \text{Im}(L \nabla \bar{L})) \cdot \Omega G \delta z - i \frac{\hbar}{2} \nabla \bar{L} \cdot \Omega \nabla L + \frac{\hbar}{2} \nabla L \cdot \Omega G \Omega \nabla \bar{L} \right] dt \\ & + \sqrt{\frac{2}{\hbar}}(\nabla L^R \cdot \delta z + \nabla L^I \cdot \Omega G \delta z)d\xi_R - \sqrt{\frac{2}{\hbar}}(\nabla L^I \cdot \delta z - \nabla L^R \cdot \Omega G \delta z)d\xi_I \Big] W. \end{aligned} \quad (23)$$

On the other hand using the Itô chain rule [34]

$$dW = \frac{\partial W}{\partial y_i} dy_i + \frac{1}{2} \frac{\partial^2 W}{\partial y_i \partial y_j} dy_i dy_j, \quad (24)$$

where

$$dy_j = \mu_j dt + \sigma_j^R d\xi_R + \sigma_j^I d\xi_I, \quad (25)$$

we have

$$\begin{aligned} dW = & \frac{\partial W}{\partial \tilde{z}_k} d\tilde{z}_k + \frac{\partial W}{\partial A_{kl}} dA_{kl} \\ & + \frac{\partial^2 W}{\partial \tilde{z}_k \partial A_{mn}} d\tilde{z}_k dA_{mn} + \frac{1}{2} \frac{\partial^2 W}{\partial \tilde{z}_k \partial \tilde{z}_l} d\tilde{z}_k d\tilde{z}_l + \frac{1}{2} \frac{\partial^2 W}{\partial A_{kl} \partial A_{mn}} dA_{kl} dA_{mn}. \end{aligned} \quad (26)$$

Here we have introduced the matrix A with $G = \frac{1}{2}(A + A^T)$, to circumvent complications arising from the symmetry condition on G . Here and for the rest of this section we implicitly sum over repeated indices (Einstein summation convention).

As we shall see, equation (26) simplifies drastically as many of the terms vanish. In particular, we find that

$$\sigma_A^R = 0 = \sigma_A^I, \quad (27)$$

and thus the second order derivatives evolving A_{jk} in equation (26) vanish. This can be seen as follows. Let us focus our attention on the term $\frac{1}{2} \frac{\partial^2 W}{\partial A_{kl} \partial A_{mn}} dA_{kl} dA_{mn}$. This term would generate a term $O(\delta z^4)$

$$\begin{aligned} \frac{1}{2} \frac{\partial^2 W}{\partial A_{kl} \partial A_{mn}} dA_{kl} dA_{mn} &= \frac{1}{2\hbar^2} ((\delta z \cdot \sigma_A^R \delta z)^2 + (\delta z \cdot \sigma_A^I \delta z)^2) dt \\ &+ \text{terms of lower order in } \delta z, \end{aligned} \quad (28)$$

which would not be matched by any term on the right hand side of equation (23), from which we infer (27). Hence equation (26) simplifies to

$$dW = \frac{\partial W}{\partial \tilde{z}_k} d\tilde{z}_k + \frac{\partial W}{\partial A_{kl}} dA_{kl} + \frac{1}{2} \frac{\partial^2 W}{\partial \tilde{z}_k \partial \tilde{z}_l} d\tilde{z}_k d\tilde{z}_l, \quad (29)$$

and we have explicitly

$$dW = \left[\frac{2}{\hbar} (\mu_z dt + \sigma_z^R d\xi_R + \sigma_z^I d\xi_I) \cdot G \delta z + \frac{1}{2} \text{Tr}(G^{-1} \mu_A) dt - \frac{1}{\hbar} \delta z \cdot \mu_A \delta z dt \right. \\ \left. - \frac{1}{\hbar} (\sigma_z^R \cdot G \sigma_z^R + \sigma_z^I \cdot G \sigma_z^I) dt + \frac{2}{\hbar^2} (\delta z \cdot G \sigma_z^R \sigma_z^{R^T} G \delta z + \delta z \cdot G \sigma_z^I \sigma_z^{I^T} G \delta z) dt \right] W. \quad (30)$$

Using $dG = \frac{1}{2}(dA + dA^T)$ and equating eqs (30) and (23) we obtain the (stochastic) dynamical equations

$$d\tilde{z} = (\Omega \nabla H + \Omega \text{Im}(L \nabla \bar{L})) dt \\ + \sqrt{\frac{\hbar}{2}} (G^{-1} \nabla L^R - \Omega \nabla L^I) d\xi_R - \sqrt{\frac{\hbar}{2}} (G^{-1} \nabla L^I + \Omega \nabla L^R) d\xi_I \quad (31)$$

$$\frac{dG}{dt} = -G \Omega H'' + H'' \Omega G + \text{Re}(\nabla \bar{L} \nabla L^T) + G \Omega \text{Re}(\nabla \bar{L} \nabla L^T) \Omega G \quad (32)$$

for the Gaussian parameters.

We notice that the deterministic part of the dynamics of the centre \tilde{z} is the same as that of the Lindblad equation, however, the SSE dynamics have an additional stochastic component as expected. This stochastic component contains covariance dependent terms and unlike in the Lindblad case we can no longer simulate the centre trajectories without calculating the covariance dynamics. For quadratic systems the evolution of the covariance matrix G is deterministic and independent of the motion of the centre, but different from that of the Lindblad evolution. This difference is not surprising taken into account that the G matrix in the SSE describes the covariances of the individual pure-state trajectories, while the G matrix of the Lindblad evolution describes that of the total density matrix arising from the ensemble average. In fact, the dynamics of G for the SSE are the same as those arising from deterministic non-Hermitian Hamiltonian dynamics, which we shall briefly review in the next section as the first phase of quantum-jump dynamics. The dynamical equation (32) for G can be explicitly solved by [26]

$$G(t) = (-\Omega \text{Re}(S(t)) \Omega G(0) + \Omega \text{Im}(S(t))) (\text{Im}(S(t)) \Omega G(0) + \text{Re}(S(t)))^{-1}, \quad (33)$$

where $S(t)$ is given by

$$S(t) = e^{\Omega(H'' - i \text{Re}(\nabla \bar{L} \nabla L^T))t}. \quad (34)$$

A short calculation also confirms that $\frac{d}{dt} \det G = 0$, implying that the Gaussian state remains pure as expected. Having obtained the evolution equations for Gaussian dynamics according to the full Lindblad and SSE dynamics, we shall now turn towards the corresponding quantum-jump dynamics.

4. Quantum-Jump dynamics

Quantum-jump dynamics do not preserve Gaussian states for arbitrary linear Lindbladians. As an example, consider the Lindblad operator $\hat{L} = \hat{a}^\dagger$. The first jump maps a state $|\psi_g\rangle$ to $\hat{a}^\dagger|\psi_g\rangle$ and thus transforms a Gaussian state into a non-Gaussian one. We will show in what follows, that it is still possible to calculate the quantum-jump dynamics building on the propagation of Gaussian states, leading again to just a handful of time-dependent parameters. For this purpose, we adapt a method developed for non-Hermitian dynamics in [19].

The quantum-jump dynamics is naturally divided into the deterministic non-Hermitian evolution interrupted by the stochastic jumps. Let us first consider the deterministic dynamics for an initially Gaussian state, which indeed remains Gaussian if the effective non-Hermitian Hamiltonian $\hat{H} - \frac{i}{2}\hat{L}^\dagger\hat{L}$ is of no higher than quadratic order in \hat{p} and \hat{q} . For simplicity, we restrict the discussion to purely quadratic (with no linear terms) effective non-Hermitian Hamiltonians $\hat{H} - \frac{i}{2}\hat{L}^\dagger\hat{L}$.

4.1. Non-Hermitian Gaussian evolution

In [35], the dynamics of a Gaussian wavepacket under a non-Hermitian Hamiltonian were derived following a similar procedure to the one we have outlined for the Lindblad and SSE cases. Substituting the effective non-Hermitian Hamiltonian into the results [35] from yields the parameter dynamics

$$\frac{d\tilde{z}}{dt} = \Omega \nabla H - G^{-1} \text{Re}(\bar{L} \nabla L) \quad (35)$$

$$\frac{dG}{dt} = -G\Omega H'' + H''\Omega G + \text{Re}(\nabla \bar{L} \nabla L^T) + G\Omega \text{Re}(\nabla \bar{L} \nabla L^T)\Omega G. \quad (36)$$

Where the evolution equation for G is the same as the one for the SSE case. As expected this fulfils $\frac{d}{dt} \det G = 0$ for $\det G = 1$, and an initially pure state remains pure. In addition, the non-Hermitian dynamics changes the normalisation N of the quantum state according to

$$\frac{dN}{dt} = \left[-\frac{1}{\hbar} \bar{L} L - \frac{1}{2} \text{Tr}(G^{-1} \text{Re}(\nabla \bar{L} \nabla L^T)) \right] N. \quad (37)$$

This equation can be integrated once the equations for \tilde{z} and G have been solved.

As has been discussed in [13] the dissipative part of the central motion of the non-Hermitian dynamics can appear either quite different or very similar to that of the Lindblad case, depending on the structure of the Lindblad operator. For a Lindblad operator that is an analytic function of \hat{a} or \hat{a}^\dagger , for example, the dissipative term in the central dynamics in equation (13), given by $\Omega \text{Im}(\bar{L} \nabla \bar{L})$ can be rewritten as $-\text{Re}(\bar{L} \nabla L)$, which is very similar to the non-Hermitian dissipation, with the difference that the latter is modulated by the changing covariance metric G . An example for which Lindblad and non-Hermitian central dynamics are very different, are Hermitian Lindbladians, for

which the dissipative term in the Lindblad dynamics vanishes entirely. The quantum-jump evolution turns the non-Hermitian behaviour into the Lindblad one, by averaging over additional quantum jumps, that in general do not leave an initially Gaussian state Gaussian.

In what follows it will be useful to consider an alternative complexified parameterisation of Gaussian states. Following a parameterisation popularised by Hagedorn [18] and utilised for non-Hermitian dynamics in [26, 19], the position representation of a Gaussian state can be expressed as

$$\psi(x, t) = \frac{1}{(\pi\hbar)^{\frac{1}{4}}(l_x(t))^{\frac{1}{2}}} \exp\left(\frac{il_p(t)}{2\hbar l_x(t)}(x - \tilde{X})^2 + \frac{i}{\hbar}\tilde{P}(x - \tilde{X})\right), \quad (38)$$

where we exchange the real parameters \tilde{z} and G for the complex ones $\tilde{Z} = \begin{pmatrix} \tilde{X} \\ \tilde{P} \end{pmatrix}$ and $l(t) = \begin{pmatrix} l_x(t) \\ l_p(t) \end{pmatrix}$. The dynamical equations of the complex parameters are then given by

$$\begin{aligned} \frac{d}{dt}\tilde{Z} &= \Omega\nabla(H - \frac{i}{2}\bar{L}L), \\ \frac{d}{dt}S &= \Omega(H - \frac{i}{2}\bar{L}L)''S = \Omega(H'' - i\operatorname{Re}(\nabla\bar{L}\nabla L^T))S, \end{aligned} \quad (39)$$

with $S(0) = \mathbb{I}$. The complex dynamics are solved by

$$\begin{aligned} S(t) &= e^{\Omega(H'' - i\operatorname{Re}(\nabla\bar{L}\nabla L^T))t}, \\ \tilde{Z}(t) &= S(t)\tilde{Z}(0), \\ l(t) &= N(t)S(t)l(0), \end{aligned} \quad (40)$$

where $N(t)$ denotes the norm of the state evolving as

$$N(t) = \left(-\frac{i}{2}l(0)^\dagger S(t)^\dagger \Omega S(t)l(0)\right)^{-\frac{1}{2}}. \quad (41)$$

The equivalent real parameters \tilde{z} and G of the Wigner function can be deduced using

$$\begin{aligned} G(t) &= -\Omega\operatorname{Re}(l_t l_t^\dagger)\Omega, \\ \tilde{z}(t) &= \operatorname{Re}\tilde{Z}(t) - \Omega G \operatorname{Im}\tilde{Z}(t). \end{aligned} \quad (42)$$

Note that the expression for $G(t)$ in equation (42) is indeed equivalent to equation (33).

4.2. Hagedorn quantum jumps

To describe the full quantum-jump dynamics we must include the effect of jumps. Since the jumps in general do not preserve Gaussian states we must use a different approach to that of the previous sections. In [19] the evolution of a complete tower of solutions to the Schrödinger dynamics generated by a quadratic non-Hermitian Hamiltonian were found that depend only on the dynamics of the complex linearised flow described by

$S(t)$ in equation (40). We will use this to deduce the full quantum-jump dynamics as follows.

We define the Hagedorn ground state centred at the origin. In the position representation, this is given by

$$\phi_G(x, t) = \frac{1}{(\pi\hbar)^{\frac{1}{4}}(l_x(t))^{\frac{1}{2}}} \exp\left(\frac{il_p(t)}{2\hbar l_x(t)}x^2\right). \quad (43)$$

For the purely quadratic cases we consider here the origin is a fixed point of the non-Hermitian centre dynamics (35), and we will use it as the centre for our dynamics.

We then define Hagedorn lowering and raising operators expressed in terms of $l(t)$ as

$$\hat{A}_t = \frac{i}{\sqrt{2\hbar}} l_t^T \Omega \hat{z} \quad \text{and} \quad \hat{A}_t^\dagger = -\frac{i}{\sqrt{2\hbar}} l_t^\dagger \Omega \hat{z}, \quad (44)$$

where \hat{z} is composed of the position and momentum operator, $\hat{z} = (\hat{x}, \hat{p})$. Although $l(0)$ may be chosen freely provided $l^\dagger(0)\Omega l(0) = 2i$ and $l^T(0)\Omega l(0) = 0$, we find it convenient to choose

$$l(0) = \begin{pmatrix} 1 \\ i \end{pmatrix}, \quad (45)$$

resulting in the ground state and the Hagedorn raising, lowering operators reducing to the familiar harmonic oscillator case at $t = 0$. The higher excited Hagedorn states are defined as

$$|\phi_k(t)\rangle = \sqrt{\frac{N(t)}{k!}} p_k \left(N_t A_t^\dagger \right) |\phi_G(t)\rangle, \quad (46)$$

with polynomials p_k of order k satisfying the recursion relation

$$p_0(t) = 1 \quad \text{and} \quad p_{k+1}(x) = x p_k(x) - m(t) p'_k(x). \quad (47)$$

Here $m(t)$ is given by

$$m(t) = \frac{l(0)^\dagger S(t)^\dagger \Omega S(t) l(0)^*}{l(0)^\dagger S(t)^\dagger \Omega S(t) l(0)}. \quad (48)$$

We should note that $|\phi_0\rangle = \sqrt{N(t)} |\phi_G\rangle$ and $|\phi_0\rangle$ evolves in both shape and norm while remaining centred at the origin. In the Hermitian Hamiltonian case, $m = 0$ and $N = 1$ for all times and the Hagedorn states reduce to the eigenstates of a (potentially squeezed) harmonic oscillator. In the non-Hermitian case, $m(t)$ may be non-zero, and thus, as time evolves the Hagedorn states acquire contributions from lower harmonic oscillator states (respecting the symmetry of the states, i.e. the even Hagedorn states only have contributions from the even harmonic oscillator states and similarly for the odd states.) The Hagedorn ladder basis $\{|\phi_k(t)\rangle\}$ does not, in general, remain orthonormal under the dynamics generated by non-Hermitian Hamiltonians. We shall discuss this further for two examples in the next section.

For a deterministic non-Hermitian evolution, a given initial state $|\psi(0)\rangle$ expanded in the basis $|\phi_k(0)\rangle$ as

$$|\psi(0)\rangle = \sum_k c_k |\phi_k(0)\rangle, \quad (49)$$

with

$$c_k = \langle \phi_k(0) | \psi(0) \rangle, \quad (50)$$

evolves in time as

$$|\psi(t)\rangle = \sum_k c_k |\phi_k(t)\rangle. \quad (51)$$

That is, the time dependence of the state is entirely encoded in the evolution of the Hagedorn states, and determined solely by the flow $S(t)$.

In the quantum-jump case, these non-Hermitian dynamics are stochastically intercepted by quantum jumps. The probability of a jump occurring at time t is encoded in the norm of the state, given by

$$\langle \psi(t) | \psi(t) \rangle = \sum_{kl} c_k^* O_{kl}(t) c_l, \quad (52)$$

where we have introduced the overlap matrix

$$O_{kl}(t) = \langle \phi_k(t) | \phi_l(t) \rangle. \quad (53)$$

Note that this norm differs from the norm $\sqrt{N_t}$ of the ground state $|\psi_0\rangle$. When a jump occurs the state $|\psi\rangle$ is mapped to

$$|\psi'\rangle = \frac{\hat{L}|\psi\rangle}{\sqrt{\langle \psi | \hat{L}^\dagger \hat{L} | \psi \rangle}}. \quad (54)$$

The denominator accounts for the renormalisation of $|\psi\rangle$ here. Expressing the Lindblad operator in the (non-orthogonal and time-dependent) basis of Hagedorn states $|\phi_k(t)\rangle$, with matrix elements L_{kl} with $L|\phi_k\rangle = \sum_l L_{kl}|\phi_l\rangle$, the jump maps

$$|\psi\rangle = \sum_k c_k |\phi_k\rangle \mapsto |\psi\rangle = \sum_k c'_k |\phi_k\rangle, \quad (55)$$

with the vector of new coefficients c' given by

$$c' = \frac{Lc}{\sqrt{c^\dagger L^\dagger O L c}}. \quad (56)$$

The coefficients after the jump are then used as the new input coefficients for the next stretch of non-Hermitian evolution until the next jump.

This can be implemented using the following algorithm, starting with an orthonormal basis $\{|\chi_k\rangle\}_k$

- (i) Discretise the time interval $(t_0, t_N) \rightarrow \{t_n\}$ with $\Delta t = t_{n+1} - t_n$;
- (ii) Calculate $S(t_n)$ and from this $\{|\phi_k(t_n)\rangle\}$, and the matrices $O(t)$ and $B(t)$ with elements $O_{kl}(t_n) = \langle \phi_k(t_n) | \phi_l(t_n) \rangle$ and $B_{jk}(t) = \langle \chi_j | \phi_k(t) \rangle$;
- (iii) Calculate the matrix representation of the Lindblad operator in the moving basis, $L = B^{-1} L_\chi B$ from the representation in the orthonormal basis L_χ ;

(iv) Find Hagedorn basis coefficients $c_k(t_0)$ of initial state $|\psi(t_0)\rangle$ using

$$c_k(t_0) = \sum_l O_{kl}^{-1}(t_0) \langle \phi_k(t_0) | \psi(t_0) \rangle ;$$

(v) Pick a uniformly distributed random number $R \sim U(0, 1)$;

(vi) For all t_n with $t_0 < t_n \leq t_N$ evaluate the following loop:

```

for k=1:N-1
    if R ≥ c(t_n)† 0(t_n) c(t_n) %Jump
        c(t_{n+1}) = L(t_n) c(t_n) / √{c†(t_n) L†(t_n) 0(t_n) L(t_n) c(t_n)} R=rand~U(0,1)
    else %No jump
        c(t_{n+1}) = c(t_n)
    end
end

```

(vii) Use $\mathbf{c}(t_n)$ to calculate the evolved state at time t_k :

$$|\psi_{t_n}\rangle = \sum_l c_l(t_n) |\phi_l(t_n)\rangle .$$

It is obvious here that while the Hagedorn method offers a unique insight into the analytical properties of the dynamics, it is of little practical benefit for speeding up numerical simulations in small systems for individual quantum-jump runs. The extra effort of propagating the whole basis set in time and calculating the overlap matrices may be compensated for if the scheme is used to generate a large number of quantum-jump trajectories since the time-dependent basis is the same for every realisation. In the examples discussed, we will nevertheless use the algorithm to implement quantum-jump trajectories numerically, to demonstrate its applicability. Its main use, however, is to guide our interpretation of the quantum-jump dynamics.

In summary, the quantum-jump dynamics for a quadratic Hamiltonian and linear Lindbladian while in general non-Gaussian, can be understood and simulated entirely on the grounds of the single dynamical quantity $S(t)$ describing the linearised complexified flow intercepted with discrete quantum jumps. In what follows we shall explore the resulting dynamics for two instructive examples.

5. Examples

To illustrate the results above, let us consider the Lindblad dynamics and the two unravellings for a harmonic oscillator Hamiltonian $\hat{H} = \frac{\omega}{2} (\hat{p}^2 + \hat{x}^2)$ with two different Lindblad operators, one Hermitian and one non-Hermitian.

5.1. Example 1: Position measurement

Let us first consider a quantum harmonic oscillator with Hermitian Lindblad operator

$$\hat{L} = \sqrt{\gamma} \hat{x}, \quad (57)$$

which can be thought of as modelling a position measurement. Since the Lindbladian is Hermitian (purely decohering), in the Lindblad dynamics it yields no contribution to the dynamics of the expectation values \tilde{z} , which simply follow the familiar harmonic oscillator trajectories. This is different for individual SSE and quantum-jump trajectories.

The dynamical equations for the Gaussian parameters in the Lindblad dynamics eq. (13) simplify to

$$\frac{d\tilde{z}}{dt} = \omega\Omega\tilde{z} \quad (58)$$

$$\frac{dG}{dt} = \omega(\Omega G - G\Omega) + 2G\Omega\Gamma\Omega G, \quad (59)$$

where we have defined

$$\Gamma = \text{Re}(\nabla L \nabla \bar{L}^T) = \begin{pmatrix} \gamma & 0 \\ 0 & 0 \end{pmatrix}. \quad (60)$$

While the central dynamics is that of the unitary harmonic oscillator, the dynamics of the covariances encoded by $G(t)$, are influenced by the position measurement. Let us consider the simple example of an initially coherent state, $G(0) = \mathbb{I}$, for which we find

$$G(t) = \frac{\omega}{d(t)} \begin{pmatrix} 2\omega(\gamma t + 1) + \gamma \sin(2\omega t) & \gamma(\cos(2\omega t) - 1) \\ \gamma(\cos(2\omega t) - 1) & 2\omega(\gamma t + 1) - \gamma \sin(2\omega t) \end{pmatrix}, \quad (61)$$

where we have defined

$$d(t) = \gamma^2(\cos(2\omega t) - 1) + 2\omega^2(\gamma t + 1)^2. \quad (62)$$

Using eq. (5) and the above we obtain the physical variances as

$$\Sigma(t) = \frac{\hbar}{2}G^{-1}(t) = \frac{\hbar}{4\omega} \begin{pmatrix} -\gamma \sin(2\omega t) + 2\omega(\gamma t + 1) & \gamma(1 - \cos(2\omega t)) \\ \gamma(1 - \cos(2\omega t)) & \gamma \sin(2\omega t) + 2\omega(\gamma t + 1) \end{pmatrix}. \quad (63)$$

That is, we observe the typical harmonic oscillations with frequency 2ω in the covariances as they appear in the unitary harmonic oscillator, accompanied by a linear growth of the position and momentum uncertainties Δx^2 and Δp^2 , associated to the effect of the position measurement. This behaviour is illustrated in figure 1 which depicts the expectation values of position and momentum and their uncertainties as a function of time for an example with $\omega = 1$ and $\gamma = 0.25$ for an initially coherent state centred at $\tilde{z}(0) = (\sqrt{2}, \sqrt{2})^T$.

The Lindblad dynamics are depicted as solid black lines.

The SSE dynamical equations (31) and (32) become

$$\begin{aligned} d\tilde{z} &= \omega\Omega\tilde{z}dt + \sqrt{\frac{\hbar\gamma}{2}} G^{-1} \begin{pmatrix} 1 \\ 0 \end{pmatrix} d\xi_R + \sqrt{\frac{\hbar\gamma}{2}} \begin{pmatrix} 0 \\ 1 \end{pmatrix} d\xi_I \\ \frac{dG}{dt} &= \omega(\Omega G - G\Omega) + \Gamma + G\Omega\Gamma\Omega G. \end{aligned} \quad (64)$$

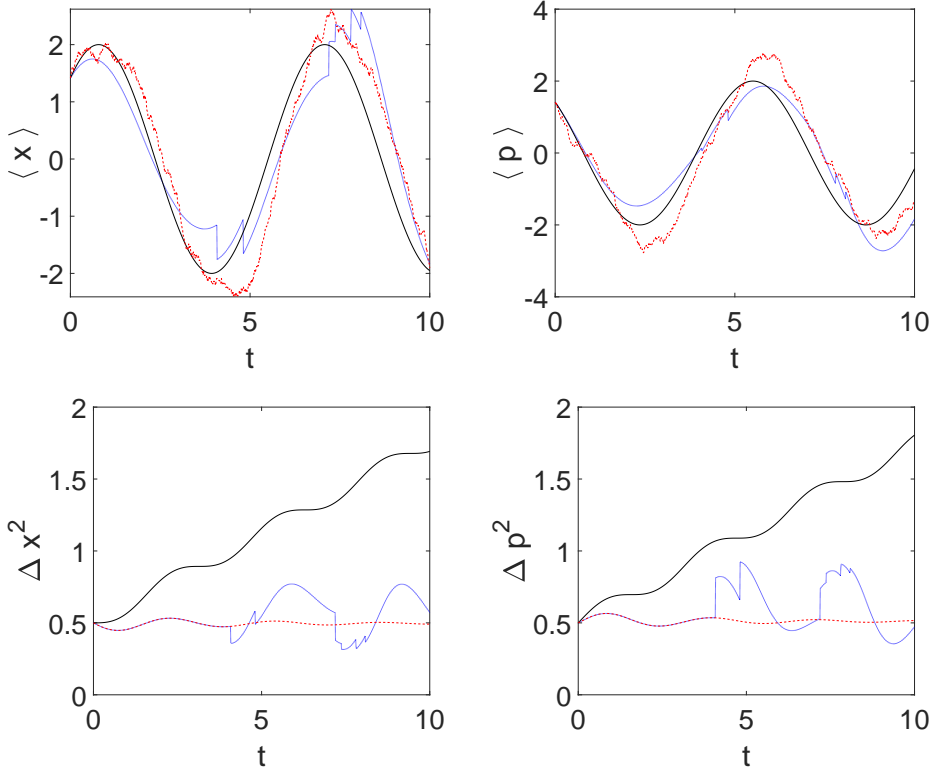


Figure 1. Lindblad dynamics (solid black line) compared with single trajectories of the SSE (dashed red line) and quantum-jump method (dotted blue line) for the position measurement model eq. (57) with $\omega = 1$ and $\gamma = 0.25$. The initial Gaussian is a coherent state (i.e. $l = (1, i)^T$ or $G = \mathbb{I}$), centered at $\tilde{z} = (\sqrt{2}, \sqrt{2})^T$. We show the time dependence of the position expectation $\langle \hat{x} \rangle$ (top left), the momentum expectation $\langle \hat{p} \rangle$ (top right), the positional variance Δx^2 (bottom left) and the momentum variance Δp^2 (bottom right).

That is, for the central motion we again have the familiar unitary Hamiltonian flow term, and no damping term, but now there is an additional width-dependent stochastic noise. The equation for the covariances differs from that in the Lindbladian case, as expected. As discussed above $G(t)$ can be solved analytically by equation (33) or (42). The linearised flow S is given by

$$S(t) = \begin{pmatrix} \cosh(\sqrt{\frac{\omega}{2}}\Lambda t) & \sqrt{\frac{\omega}{2\lambda^2}}\Lambda^* \sinh(\sqrt{\frac{\omega}{2}}\Lambda t) \\ \sqrt{\frac{1}{2\omega}}\Lambda \sinh(\sqrt{\frac{\omega}{2}}\Lambda t) & \cosh(\sqrt{\frac{\omega}{2}}\Lambda t) \end{pmatrix}, \quad (65)$$

where we have defined

$$\lambda = \sqrt{\gamma^2 + \omega^2} \quad \text{and} \quad \Lambda = \sqrt{\lambda - \omega} + i\sqrt{\lambda + \omega}. \quad (66)$$

That is, we have an oscillatory contribution with frequency $\sqrt{\frac{\omega(\lambda+\omega)}{2}}$, which reduces to oscillations with frequency ω in the limit $\gamma = 0$, and an additional exponential growth

with rate $\sqrt{\lambda - \omega}$. The asymptotic behaviour for large times is given by

$$\lim_{t \rightarrow \infty} S(t) = e^{\sqrt{\frac{\omega}{2}} \Lambda t} \begin{pmatrix} 1 & \sqrt{\frac{\omega}{2\lambda^2}} \Lambda^* \\ \sqrt{\frac{1}{2\omega}} \Lambda & 1 \end{pmatrix}. \quad (67)$$

As a result, independent of the initial value, $G(t)$ tends to a fixed point as $t \rightarrow \infty$ given by

$$G(t) \rightarrow \frac{1}{\gamma} \begin{pmatrix} \frac{\lambda}{\sqrt{\omega}} \sqrt{2(\lambda - \omega)} & (\omega - \lambda) \\ (\omega - \lambda) & \sqrt{2\omega(\lambda - \omega)} \end{pmatrix}. \quad (68)$$

This is in stark contrast to the behaviour of the Lindblad covariances, with their linear growth in Δx^2 and Δp^2 . The limiting behaviour is clearly observable in the example in figure 1, which shows the SSE dynamics as red dashed lines. For the central dynamics we observe stochastic fluctuations around the average Lindblad dynamics.

The quantum-jump trajectories, on the other hand, depicted as blue dotted lines in figure 1, show a very different behaviour. Here up to the first jump, the centre of the Gaussian state follows the non-Hermitian dynamics, which in the present case reduce to

$$\frac{d\tilde{z}}{dt} = \omega \Omega \tilde{z} - \gamma G^{-1} \begin{pmatrix} x \\ 0 \end{pmatrix}, \quad (69)$$

where $G(t)$ evolves dynamically as in the SSE case. That is, there is an additional damping term, modulated by the covariances of the state. This is clearly visible in the example depicted in figure 1, in both the dynamics of the position and the momentum expectation values, which perform a deterministic damped oscillation until the first jump. We also observe that, as expected, the dynamics of position and momentum uncertainties agree between the Hagedorn jump and the SSE dynamics up to the first jump. What is not shown here, but has been numerically verified, is that averaging over many trajectories for the case of the Hagedorn quantum jumps and the Gaussian SSE does indeed recover the Lindblad dynamics.

In figure 2 we depict the Wigner functions of the quantum-jump trajectory for the same realisation as in figure 1 at three selected times, where the central trajectory up to this time is depicted as a solid white line. The damped Gaussian motion is clearly visible in the first figure, just before the first jump in this realisation. The remaining figures illustrate the effect of the quantum jumps, resulting in a sudden displacement of the centre as well as the expected deviations from a Gaussian state. At the jump the state is acted on by the position operator and the resulting state is no longer Gaussian. We clearly observe interference patterns in the Wigner function corresponding to the excitation of higher harmonic oscillator states. It is remarkable that averaging over these non-classical excited states results in the same Gaussian state as the Lindblad equation.

Numerically, we have not used the non-Hermitian Gaussian evolution up to the first jump but instead have expressed our initial state in a Hagedorn basis centred at the origin, which is a fixed point of the dynamics. That is, the initial Gaussian

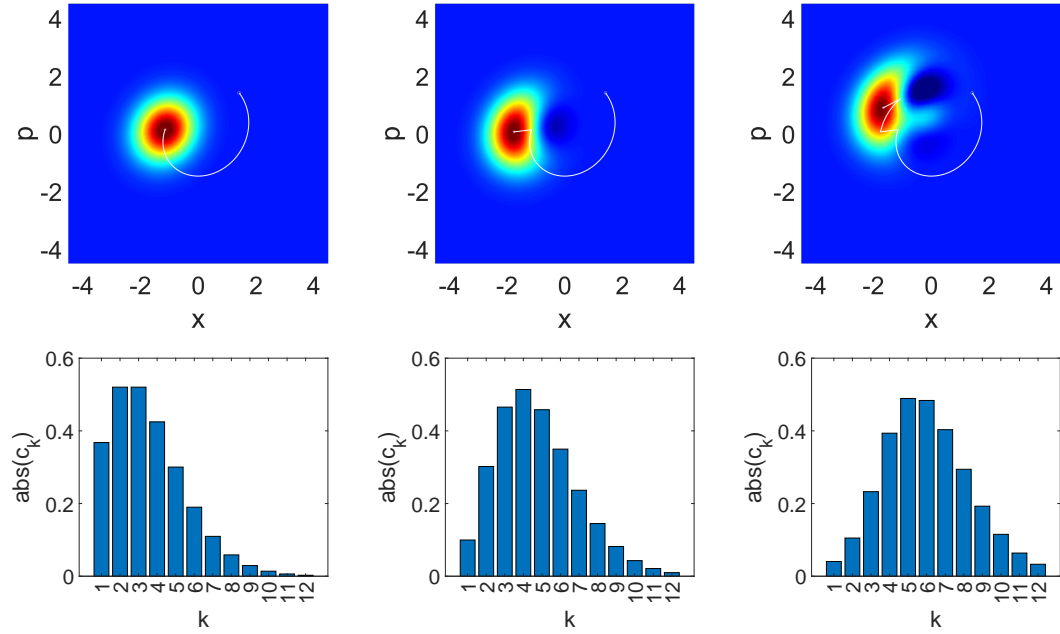


Figure 2. Top row: Wigner functions of a single trajectory of the Hagedorn jump method corresponding to the dynamics in figure 1 at selected times (from left to right: $t=4.08$ (shortly before the first jump) and $t=4.09$ (just after the first jump) and $t=4.82$ (just after the second jump)). The white line traces the preceding central motion. Bottom row: Magnitudes of the coefficients of the state in the Hagedorn basis ($|c_k|$) at the same times as in the top row.

does not correspond to an individual basis state in this implementation, but instead a superposition of many basis states. The coefficients of the initial Gaussian in this basis are depicted in the histogram in the left bottom panel of figure 2. The choice of centering the basis in the fixed point of the dynamics ensures that the phase-space centers of individual basis states remain fixed in the same location. This does not mean that a linear combination of basis states will remain fixed in phase space as the basis states change shape over time. The change in shape of each of the basis states is illustrated for the first four basis states in figure 3, which depicts the Wigner functions of these four states at times $t = 0, 5$ and $t = 10$.

Analytically the evolution of the basis states is solely described by the linearized flow in equation (65). We may use this expression together with eqs. (41) and (48) to calculate $N(t)$ and $m(t)$. Note that the dynamics of $N(t)$ and $m(t)$ do not depend on the initial position of the wavepacket, but solely on the values of ω and γ . Using the asymptotic behaviour of $S(t)$ we find that $N(t)$ for long times follows a simple exponential decay

$$N(t) \rightarrow \exp\left(-\sqrt{\frac{\omega(\lambda - \omega)}{2}}t\right), \quad (70)$$

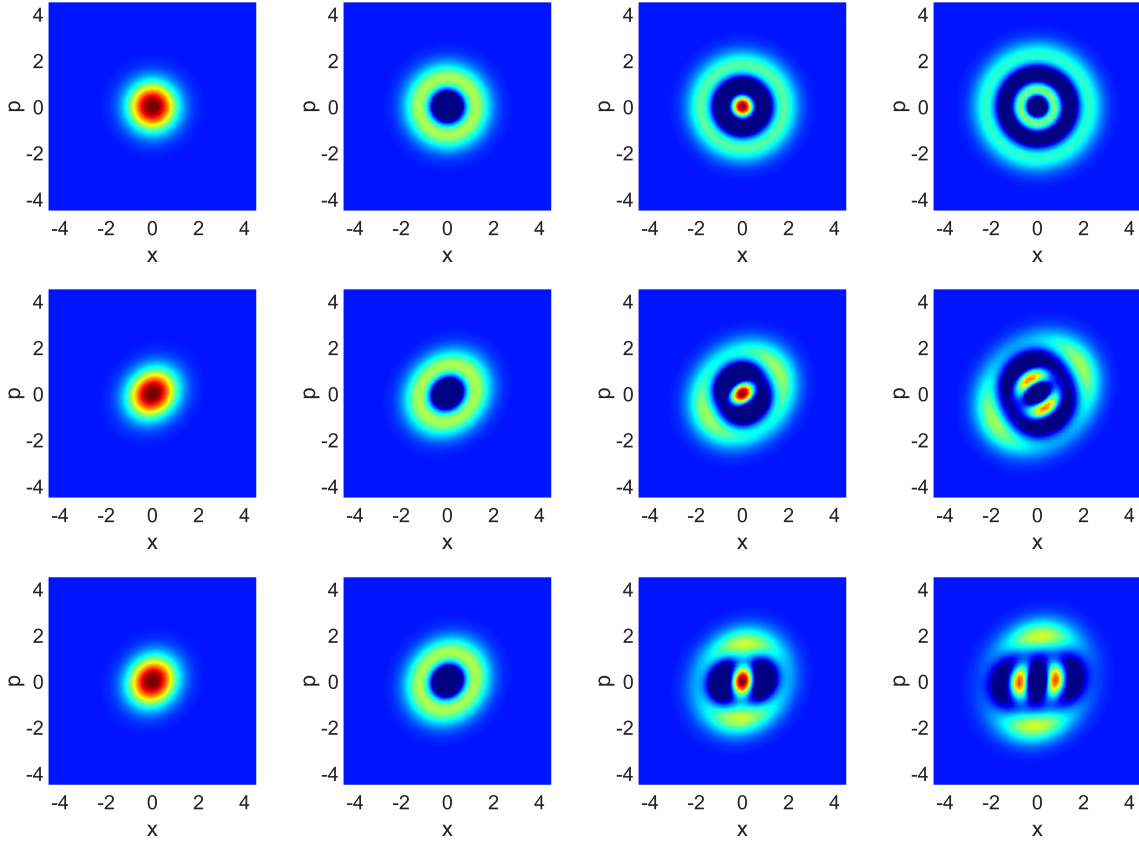


Figure 3. Wigner functions of the first four Hagedorn states (from state 0 to state 4 from left to right) at times $t = 0, 5, 10$ (top to bottom)

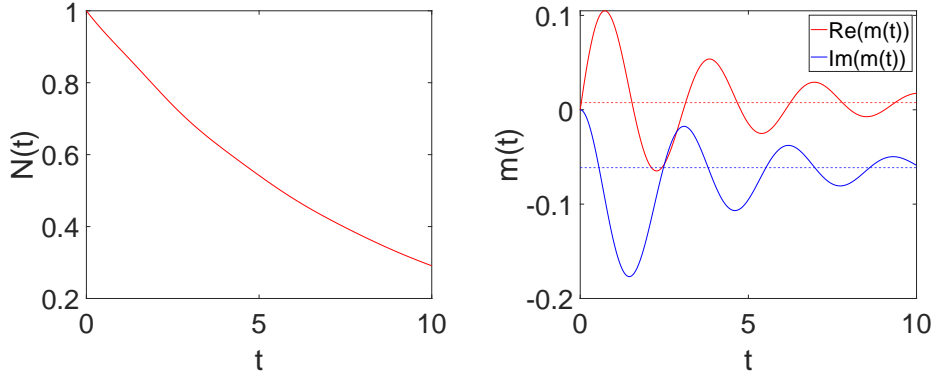


Figure 4. Parameter evolution for the Hagedorn quantum-jump method. The figure on the left shows the norm $N(t)$ of the ground state, the right figure the evolution of the parameter $m(t)$ determining the behaviour of the Hagedorn basis states.

while $m(t)$ tends to the fixed value

$$m(t) \rightarrow 1 - \sqrt{\frac{2\omega}{\lambda + \omega}} + i \left(\frac{2\omega - \sqrt{2\omega(\lambda + \omega)}}{\sqrt{(\lambda - \omega)(\lambda + \omega)}} \right). \quad (71)$$

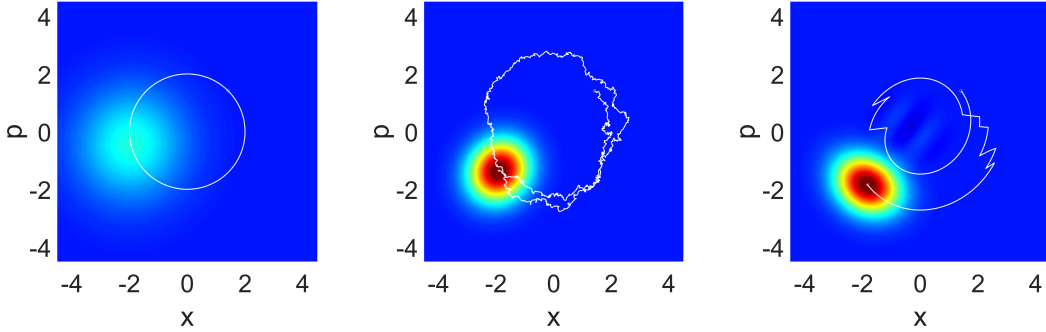


Figure 5. Lindblad dynamics compared with a single trajectory of the Hagedorn jump method and Gaussian SSE for the position measurement model eq. (57), with parameters $\omega = 1$ and $\gamma = 0.25$. The initial coherent state with $\tilde{z} = (\sqrt{2}, \sqrt{2})^T$. In each case a snapshot of the Wigner function at $t = 10$ is plotted in phase space, with a white line displaying the precedent central motion. The left plot corresponds to the quantum-jump dynamics, the middle one to the SSE and the right plot to the Lindblad dynamics.

The dynamics of $N(t)$ and $m(t)$ for the example considered here are depicted in figure 4. We clearly observe the expected decay in the ground state normalisation and the approach to the fixed point value in $m(t)$.

The Hagedorn raising operator A_t^\dagger (eq. (44)) is also determined by $S(t)$ and in the long time limit it takes the form

$$A_t^\dagger \rightarrow \frac{e^{\frac{i}{2}(\sqrt{\lambda+\gamma}+\sqrt{\lambda-\gamma})t}}{\sqrt{2\hbar}} \left(\left(1 + i\sqrt{\frac{\omega}{2\lambda^2}}\Lambda \right) \hat{x} - \left(1 + \sqrt{\frac{\omega}{2}}\Lambda^* \right) i\hat{p} \right). \quad (72)$$

Which we recognise as the re-scaled harmonic oscillator creation operator with a rotating phase of angular frequency $\frac{1}{2}(\sqrt{\lambda+\gamma} + \sqrt{\lambda-\gamma})$.

These quantities determine the time evolution of the Hagedorn basis states, the first four of which are depicted for different times in fig. 3. We observe the beginning of the decay of the second Hagedorn state into the ground state and the third Hagedorn state into the first one, modulated both by $N(t)$ and $m(t)$. We also note the rotation and squeezing induced by \hat{A}_t^\dagger . Note that the evolution of the Hagedorn basis states do not depend on the specific realisation of the quantum-jump trajectory. What differs between different quantum-jump realisations are the coefficients of the state in this basis. For a given initial state they remain constant between the jumps and are updated at each jump according to equation (56). The coefficients for our example just before and just after the first jump, and just after the second jump are depicted in the bottom row of figure 2.

To summarise, we observe clear differences between the Lindblad, SSE and quantum-jump dynamics for the harmonic oscillator with position measurement, which can be understood to a large degree using the analytical treatment developed in the previous sections. Figure 5 shows the Wigner functions of the state at $t = 10$ for the three different realisations together with the central trajectory up until this time. In the

right panel, corresponding to the Lindblad dynamics the state remains Gaussian, and its central motion follows the usual unitary harmonic oscillator trajectory. The increased uncertainties in position and momentum lead to the broadening of the Gaussian apparent here. The SSE dynamics in the central picture, on the other hand, also remains Gaussian in shape and stays well localised as predicted by the dynamical behaviour of G . The central trajectory performs a Brownian motion around the harmonic oscillator trajectory. Finally, the quantum-jump trajectory performs smooth stretches of damped harmonic oscillations interrupted by discrete jumps, and crucially, the state does not remain Gaussian.

5.2. Example 2: Damped harmonic oscillator

As a second example we consider again a harmonic oscillator Hamiltonian and the non-Hermitian Lindbladian

$$\hat{L} = \sqrt{\hbar\gamma}\hat{a} = \sqrt{\frac{\gamma}{2}}(\hat{x} + i\hat{p}). \quad (73)$$

For an initially coherent state, the resulting dynamics are rather trivial, as such a state is an eigenstate of both the Hamiltonian and the Lindbladian. As a result, for both the quantum-jump and SSE the stochastic terms vanish and the dynamics of all three descriptions is the same, simply transporting the initial state along the trajectories of the damped oscillator. Using a squeezed initial state instead, the motion becomes more interesting and Lindblad, SSE and quantum-jump trajectories differ.

Explicitly the dynamical equations for the Lindblad evolution eq. (13) become

$$\begin{aligned} \frac{d\tilde{z}}{dt} &= \omega\Omega\tilde{z} - \frac{\gamma\tilde{x}}{2} \begin{pmatrix} 1 \\ 0 \end{pmatrix} \\ \frac{dG}{dt} &= \omega(\Omega G - G\Omega) + \gamma(G - G^2). \end{aligned} \quad (74)$$

The equation for the central dynamics is simply that of a damped oscillator. It can be written in terms of a second-order differential equation for \tilde{x} taking the more familiar form

$$\frac{d^2\tilde{x}}{dt^2} + \frac{\gamma}{2} \frac{d\tilde{x}}{dt} + \omega^2\tilde{x} = 0. \quad (75)$$

Thus, the central dynamics is given by

$$\begin{pmatrix} \tilde{x}(t) \\ \tilde{p}(t) \end{pmatrix} = e^{-\frac{\gamma t}{4}} \begin{pmatrix} \tilde{x}(0) \cosh\left(\frac{1}{4}\sqrt{\gamma^2 - 16\omega^2}t\right) + \frac{-\gamma\tilde{x}(0) + 4\omega\tilde{p}(0)}{\sqrt{\gamma^2 - 16\omega^2}} \sinh\left(\frac{1}{4}\sqrt{\gamma^2 - 16\omega^2}t\right) \\ \tilde{p}(0) \cosh\left(\frac{1}{4}\sqrt{\gamma^2 - 16\omega^2}t\right) + \frac{\gamma\tilde{p}(0) - 4\omega\tilde{x}(0)}{\sqrt{\gamma^2 - 16\omega^2}} \sinh\left(\frac{1}{4}\sqrt{\gamma^2 - 16\omega^2}t\right) \end{pmatrix}. \quad (76)$$

In the equation for the covariance matrix G we immediately observe the fixed point for $G = \mathbb{I}$, corresponding to a coherent state, which is indeed approached asymptotically by any initial Gaussian state. For an initially squeezed state with $G(0) = \begin{pmatrix} \eta & 0 \\ 0 & 1/\eta \end{pmatrix}$ we

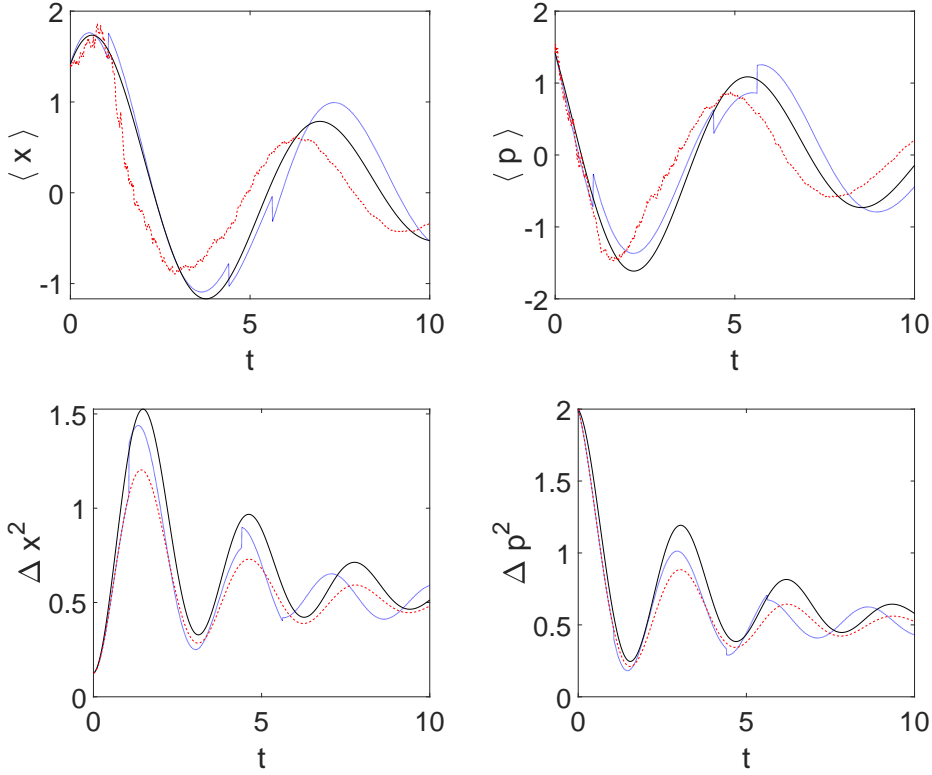


Figure 6. Lindblad dynamics (solid black line) compared with single trajectories of the SSE (dashed red line) and quantum-jump method (dotted blue line) for the damped oscillator model eq. (73) with $\omega = 1$ and $\gamma = 0.25$. The initial Gaussian is a squeezed state with $G = \begin{pmatrix} 4 & 0 \\ 0 & \frac{1}{4} \end{pmatrix}$, centered at $\tilde{z} = (\sqrt{2}, \sqrt{2})^T$. We show the time dependence of the position expectation $\langle \hat{x} \rangle$ (top left), the momentum expectation $\langle \hat{p} \rangle$ (top right), the positional variance Δx^2 (bottom left) and the momentum variance Δp^2 (bottom right).

find the covariances

$$\Sigma(t) = \frac{\hbar}{2} \begin{pmatrix} 1 & 0 \\ 0 & 1 \end{pmatrix} + \frac{\hbar e^{-\gamma t}}{4\eta} \begin{pmatrix} (\eta - 1)^2 - (\eta^2 - 1) \cos(2\omega t) & (\eta^2 - 1) \sin(2\omega t) \\ (\eta^2 - 1) \sin(2\omega t) & (\eta - 1)^2 + (\eta^2 - 1) \cos(2\omega t) \end{pmatrix} \quad (77)$$

That is, we observe the usual oscillations with frequency 2ω around the coherent state covariances, which are now damped, and $\Sigma(t)$ asymptotically approaches $\Sigma(t) \rightarrow \frac{\hbar}{2}\mathbb{I}$, while $\tilde{z} \rightarrow (0, 0)^T$, resulting in a coherent state at the origin. This behaviour is clearly visible in figure 6, in which the expectation values and uncertainties of position and momentum in the Lindblad case are depicted as black solid lines for an initial state with $\eta = 4$ centred at $\tilde{z}_0 = (\sqrt{2}, \sqrt{2})^T$.

The dynamical eqs. (31) and (32) in the SSE case become

$$\begin{aligned} \frac{d\tilde{z}}{dt} &= \omega\Omega\tilde{z}dt - \frac{\gamma\tilde{x}}{2} \begin{pmatrix} 1 \\ 0 \end{pmatrix} dt + \frac{\sqrt{\hbar\gamma}}{2} (G^{-1} - \mathbb{I}) \begin{pmatrix} 1 \\ 0 \end{pmatrix} d\xi_R - \frac{\sqrt{\hbar\gamma}}{2} (G^{-1} - \mathbb{I}) \begin{pmatrix} 0 \\ 1 \end{pmatrix} d\xi_I \quad (78) \\ \frac{dG}{dt} &= \omega(\Omega G - G\Omega) + \frac{\gamma}{2}(\mathbb{I} - G^2). \end{aligned}$$

The deterministic part of the SSE and the Lindblad central dynamics agree as usual. The additional drift term is proportional to $G^{-1} - \mathbb{I}$, and vanishes for the coherent state $G = \mathbb{I}$. Although the evolution of G differs from the Lindblad case, it too asymptotically approaches the fixed point $G = \mathbb{I}$, independent of the initial conditions. Thus, the stochastic contributions to the central trajectory become smaller over time, and the dynamics ten in a coherent state in the centre, just as in the Lindblad case.

The complexified linearised flow of the damped oscillator model eq. (73) is explicitly given by

$$S(t) = \begin{pmatrix} \cosh\left(\frac{\gamma+2i\omega}{2}t\right) & -i \sinh\left(\frac{\gamma+2i\omega}{2}t\right) \\ i \sinh\left(\frac{\gamma+2i\omega}{2}t\right) & \cosh\left(\frac{\gamma+2i\omega}{2}t\right) \end{pmatrix}, \quad (79)$$

For an initial state with $G(0) = \begin{pmatrix} \eta & 0 \\ 0 & 1/\eta \end{pmatrix}$ this yields the time dependent covariances in the SSE dynamics

$$\Sigma(t) = \frac{\hbar}{2f(t)} \begin{pmatrix} (\eta^2+1) \cosh(\gamma t) + 2\eta \sinh(\gamma t) - (\eta^2-1) \cos(2\omega t) & (\eta^2-1) \sin(2\omega t) \\ (\eta^2-1) \sin(2\omega t) & (\eta^2+1) \cosh(\gamma t) + 2\eta \sinh(\gamma t) + (\eta^2-1) \cos(2\omega t) \end{pmatrix}, \quad (80)$$

with

$$f(t) = (\eta^2 + 1) \sinh(\gamma t) + 2\eta \cosh(\gamma t). \quad (81)$$

For long times $t \rightarrow \infty$ this behaves as

$$\Sigma(t) = \frac{\hbar}{2} \begin{pmatrix} 1 & 0 \\ 0 & 1 \end{pmatrix} + \frac{\hbar(\eta-1)}{2(1+\eta)} e^{-\gamma t} \begin{pmatrix} -\cos(2\omega t) & \sin(2\omega t) \\ \sin(2\omega t) & \cos(2\omega t) \end{pmatrix}, \quad (82)$$

with $\Sigma(t)$ approaching $\frac{\hbar}{2}\mathbb{I}$ just as in the Lindblad case. The example in figure 6 nicely demonstrates how the SSE and Lindblad dynamics approach the same limit in different ways. We also observe the reduced amplitude of the noise in the central dynamics, as the matrix G approaches the identity.

The Hagedorn quantum jump in this example again initially follows the Gaussian dynamics, here given by

$$\frac{d\tilde{z}}{dt} = (\omega\Omega - \gamma G^{-1}) \tilde{z}, \quad (83)$$

where $G(t)$ evolves dynamically as in the SSE case. This central dynamics is also a type of damped harmonic oscillator, however, it differs from the Lindblad case, both in the presence of a damping term in both position and momentum, and in the modulation of the damping induced by the time-dependent covariance matrix. In the example in figure 6, however, we observe that this is a quantitative rather than qualitative difference in this case.

The full Hagedorn quantum-jump dynamics also simplifies in the present case, with the dynamical variables given by

$$\begin{aligned} N(t) &= e^{-\frac{\gamma}{2}t}, \\ l(t) &= e^{i\omega t} \begin{pmatrix} 1 \\ i \end{pmatrix}, \\ m(t) &= 0, \end{aligned} \quad (84)$$

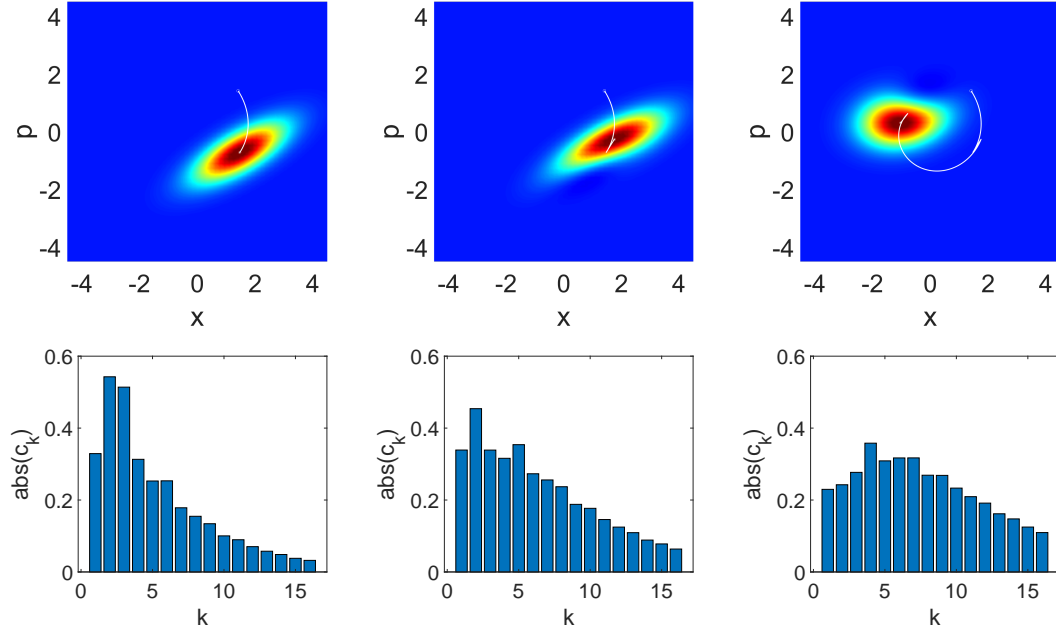


Figure 7. Top row: Wigner functions of a single trajectory of the Hagedorn jump method corresponding to the dynamics in figure 1 at selected times (from left to right: $t=1.06$ (shortly before the first jump) and $t=1.07$ (just after the first jump) and $t=4.07$ (just after the second jump)). The white line traces the preceding central motion. Bottom row: Magnitudes of the coefficients of the state in the Hagedorn basis ($|c_k|$) at the same times as in the top row.

using eqs. (40), (41) and (48) respectively. That is, in position representation our Hagedorn ground state is given by

$$\phi_G(x, t) = (\pi\hbar)^{-\frac{1}{4}} \exp\left(\frac{i\omega t}{2}\right) \exp\left(-\frac{x^2}{2\hbar}\right), \quad (85)$$

which remains a coherent state for all times, with phase that rotates with the harmonic oscillation as $\frac{\omega}{2}t$. Also the Hagedorn raising operator A_t^\dagger evolves only in the same phase, and is given by

$$A_t^\dagger = e^{-i\omega t} \hat{a}^\dagger, \quad (86)$$

Where \hat{a}^\dagger is the standard harmonic oscillator raising operator $\hat{a}^\dagger = \frac{1}{\sqrt{2\hbar}}(\hat{x} - i\hat{p})$. Most importantly, since $m(t) = 0$ for all times, the time-dependent Hagedorn states eq. (46) are simply given by

$$\begin{aligned} |\phi_k(t)\rangle &= \sqrt{\frac{N_t}{k!}} \left(N_t A_t^\dagger\right)^k |\phi_G(t)\rangle \\ &= \exp\left(-i\omega(k-1)t - \frac{\gamma}{4}(2k+1)t\right) |k\rangle, \end{aligned} \quad (87)$$

where $|k\rangle$ denotes the harmonic oscillator eigenstates. These states remain orthogonal for all times, but the norm of the higher states decays leading to an effective decay of the overall state towards the ground state centered at $z = (0, 0)^T$ in between jumps.

The overlap matrix eq. (53) of the Hagedorn states and change of basis matrix from the standard harmonic oscillator basis are diagonal, with diagonal elements given by

$$O_{kl} = \exp\left(-\frac{\gamma}{2}(2k+1)t\right)\delta_{kl} \quad \text{and} \quad B_{kl} = \exp\left(-i\omega(k-1)t - \frac{\gamma}{4}(2k+1)t\right)\delta_{kl}. \quad (88)$$

Since B is a diagonal matrix it is easily inverted and may be used to write the matrix representation of the Lindbladian in the moving basis as

$$\begin{aligned} L_{kl} &= B_{ki}^{-1} L_{ij}^{\text{HO}} B_{jl} \\ &= \exp\left(-i\omega(l-k)t - \frac{\gamma}{2}(l-k)t\right) \langle k | \hat{L} | l \rangle \\ &= \exp\left(-i\omega t - \frac{\gamma}{2}t\right) \sqrt{\gamma(k+1)} \delta_{k+1,l} \end{aligned} \quad (89)$$

That is, the jump updates the coefficients as in eq. (56)

$$c'_k = \frac{\exp\left(-i\omega t - \frac{\gamma}{2}t\right) \sqrt{\gamma(k+1)} c_{k+1}}{\sqrt{\sum_k \exp\left(-\frac{\gamma}{2}(2k+3)t\right) \gamma(k+1) |c_{k+1}|^2}} \quad (90)$$

The jumps interrupt the decay into the centre and can momentarily displace the state further away from the asymptotic one, but eventually, as the state becomes closer to the coherent state, their contribution becomes less significant. Figure 7 illustrates the effect of the first two jumps in the particular realisation of figure 6, showing the Wigner distributions shortly before the first jump and shortly after the first and second jumps, as well as the corresponding coefficients in the Hagedorn basis. In the Wigner function, we observe how the state after two jumps is significantly closer to a circular coherent state already, this effect results from a combination of the jump terms and the damped motion between the jumps.

Figure 8 depicts the Wigner functions of the Lindblad, SSE and quantum-jump dynamics at time $t = 10$, as well as the corresponding central trajectory up to this time. In comparison with the previous example, we now see dissipation for all three dynamics. The effect of the diminishing stochastic contribution in the SSE dynamics, specific to the Lindbladian considered here, is also visible in the figure. While the final quantum-jump state is still non-Gaussian, every individual run asymptotically approaches a coherent state in the centre, in contrast to the dynamics resulting from the first example.

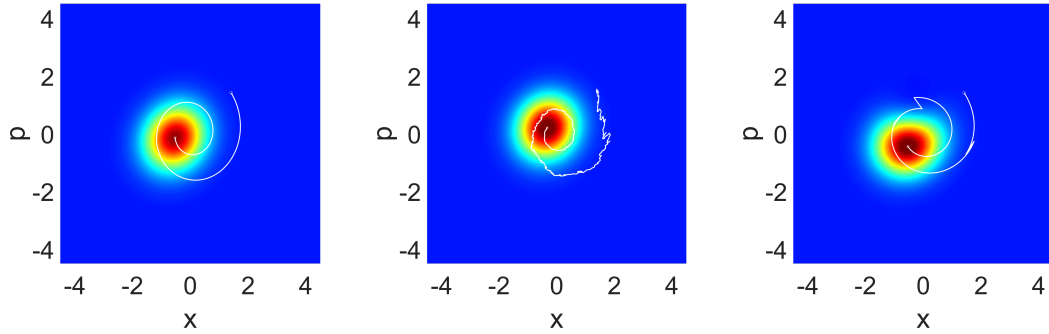


Figure 8. Lindblad dynamics compared with a single trajectory of the Hagedorn jump method and Gaussian SSE for the position measurement model eq. (73) as in figure 6. In each case, a snapshot of the Wigner function at $t = 10$ is plotted in phase space, with a white line displaying the precedent central motion. The left plot corresponds to the quantum-jump dynamics, the middle one to the SSE and the right plot to the Lindblad dynamics.

6. Summary and outlook

We have investigated the dynamics of initially Gaussian states in open quantum systems described in a Lindblad formalism with a quadratic Hamiltonian and linear Lindbladian in comparison to the two popular unravellings of the dynamics given by SSE and quantum-jump trajectories. In the SSE case, the state remains Gaussian for all times, where the central dynamics has a possibly damped deterministic contribution accompanied by a stochastic term that depends on the covariances of the state. The covariances themselves follow a deterministic time evolution, that is independent of the central trajectory, and that coincides with the dynamical equation found for quantum evolution generated by an effective non-Hermitian Hamiltonian. For the quantum-jump approach, initial Gaussian states do in general not stay Gaussian over time. Applying results from [19] we have formulated a method to describe quantum-jump trajectories utilising a family of solutions to the non-Hermitian Schrödinger equation that depends only on the dynamics of a 2×2 complex matrix known as the linearised flow. We have studied the similarities and differences of the dynamics resulting in the SSE, the quantum-jump and the Lindblad descriptions for two important examples.

For the Hagedorn quantum-jump approach we utilised a basis centred at the fixed point of the dynamics, and while this was useful for an interpretation of the dynamics, it led to a high numerical cost for the simulation of individual quantum-jump trajectories, as compared to a direct implementation of a quantum-jump algorithm. In the future we are hoping to extend the Hagedorn jump method to allow the centre of the ladder of states (z_0) to move with the centre of the initial wavepacket, minimising the number of basis elements $|\phi_k(t)\rangle$ needed to accurately represent a state.

7. Acknowledgements

We would like to thank Bradley Longstaff for his time checking calculations of the SSE Gaussian limit as well as Roman Schubert for enlightening correspondence regarding Hagedorn wavepackets.

We acknowledge support from the Royal Society (Grants. No. URF\R\201034 and RGF\EA\180169) and from the European Research Council (ERC) under the European Union's Horizon 2020 research and innovation programme (grant agreement No 758453).

8. References

- [1] H. M. Wiseman and G. J. Milburn, *Quantum measurement and control*. Cambridge university press, 2009.
- [2] V. P. Belavkin, "Nondemolition measurements, nonlinear filtering and dynamic programming of quantum stochastic processes," in *Modeling and Control of Systems*. Springer, 1989, pp. 245–265.
- [3] H. Carmichael, *An open systems approach to quantum optics: lectures presented at the Université Libre de Bruxelles, October 28 to November 4, 1991*. Springer Science & Business Media, 2009, vol. 18.
- [4] N. Bartolo, F. Minganti, J. Lolli, and C. Ciuti, "Homodyne versus photon-counting quantum trajectories for dissipative kerr resonators with two-photon driving," *The European Physical Journal Special Topics*, vol. 226, no. 12, pp. 2705–2713, 2017.
- [5] J. K. Eastman, J. J. Hope, and A. R. Carvalho, "Tuning quantum measurements to control chaos," *Scientific reports*, vol. 7, no. 1, pp. 1–10, 2017.
- [6] H. Wiseman, "Quantum trajectories and quantum measurement theory," *Quantum and Semiclassical Optics: Journal of the European Optical Society Part B*, vol. 8, no. 1, p. 205, 1996.
- [7] M. B. Plenio and P. L. Knight, "The quantum-jump approach to dissipative dynamics in quantum optics," *Reviews of Modern Physics*, vol. 70, no. 1, p. 101, 1998.
- [8] G. C. Ghirardi, A. Rimini, and T. Weber, "Unified dynamics for microscopic and macroscopic systems," *Physical review D*, vol. 34, no. 2, p. 470, 1986.
- [9] A. Bassi, K. Lochan, S. Satin, T. P. Singh, and H. Ulbricht, "Models of wave-function collapse, underlying theories, and experimental tests," *Reviews of Modern Physics*, vol. 85, no. 2, p. 471, 2013.
- [10] D. C. Brody and L. P. Hughston, "Efficient simulation of quantum state reduction," *Journal of Mathematical Physics*, vol. 43, no. 11, pp. 5254–5261, 2002.
- [11] N. Gisin and I. C. Percival, "The quantum-state diffusion model applied to open systems," *Journal of Physics A: Mathematical and General*, vol. 25, no. 21, p. 5677, 1992.
- [12] O. Brodier and A. Ozorio de Almeida, "Symplectic evolution of wigner functions in markovian open systems," *Phys. Rev. E*, vol. 69, p. 016204, 2004.
- [13] E. Graefe, B. Longstaff, T. Plastow, and R. Schubert, "Lindblad dynamics of Gaussian states and their superpositions in the semiclassical limit," *Journal of Physics A: Mathematical and Theoretical*, vol. 51, no. 36, p. 365203, 2018.
- [14] E. J. Heller, "Time-dependent approach to semiclassical dynamics," *The Journal of Chemical Physics*, vol. 62, no. 4, pp. 1544–1555, 1975.
- [15] R. G. Littlejohn, "The semiclassical evolution of wave packets," *Physics reports*, vol. 138, no. 4–5, pp. 193–291, 1986.
- [16] W. T. Strunz and I. C. Percival, "Classical mechanics from quantum state diffusion-a phase-space approach," *Journal of Physics A: Mathematical and General*, vol. 31, no. 7, p. 1801, 1998.

- [17] J. Halliwell and A. Zoupas, “Quantum state diffusion, density matrix diagonalization, and decoherent histories: A model,” *Physical Review D*, vol. 52, no. 12, p. 7294, 1995.
- [18] G. A. Hagedorn, “Raising and lowering operators for semiclassical wave packets,” *Annals of Physics*, vol. 269, no. 1, pp. 77–104, 1998.
- [19] C. Lasser, R. Schubert, and S. Troppmann, “Non-hermitian propagation of hagedorn wavepackets,” *Journal of Mathematical Physics*, vol. 59, no. 8, p. 082102, 2018.
- [20] V. Gorini, A. Kossakowski, and E. C. G. Sudarshan, “Completely positive dynamical semigroups of n-level systems,” *Journal of Mathematical Physics*, vol. 17, no. 5, pp. 821–825, 1976.
- [21] G. Lindblad, “On the generators of quantum dynamical semigroups,” *Communications in Mathematical Physics*, vol. 48, no. 2, pp. 119–130, 1976.
- [22] H.-P. Breuer, F. Petruccione *et al.*, *The theory of open quantum systems*. Oxford University Press on Demand, 2002.
- [23] A. J. Daley, “Quantum trajectories and open many-body quantum systems,” *Advances in Physics*, vol. 63, no. 2, pp. 77–149, 2014.
- [24] F. Klauck, L. Teuber, M. Ornigotti, M. Heinrich, S. Scheel, and A. Szameit, “Observation of pt-symmetric quantum interference,” *Nature Photonics*, vol. 13, no. 12, pp. 883–887, 2019.
- [25] E.-M. Graefe, “PT symmetry dips into two-photon interference,” *Nature Photonics*, vol. 13, no. 12, pp. 822–823, 2019.
- [26] E.-M. Graefe and R. Schubert, “Complexified coherent states and quantum evolution with non-hermitian hamiltonians,” *Journal of Physics A: Mathematical and Theoretical*, vol. 45, no. 24, p. 244033, 2012.
- [27] R. L. Hudson, “When is the Wigner quasi-probability density non-negative?” *Reports on Mathematical Physics*, vol. 6, no. 2, pp. 249–252, 1974.
- [28] A. Kenfack and K. Życzkowski, “Negativity of the Wigner function as an indicator of non-classicality,” *Journal of Optics B: Quantum and Semiclassical Optics*, vol. 6, no. 10, p. 396, 2004.
- [29] P. de M Rios and A. O. de Almeida, “On the propagation of semiclassical wigner functions,” *Journal of Physics A: Mathematical and General*, vol. 35, no. 11, p. 2609, 2002.
- [30] W. T. Strunz, “Path integral, semiclassical and stochastic propagators for markovian open quantum systems,” *Journal of Physics A: Mathematical and General*, vol. 30, no. 11, p. 4053, 1997.
- [31] W. T. Strunz, L. Diósi, N. Gisin, and T. Yu, “Quantum trajectories for brownian motion,” *Physical Review Letters*, vol. 83, no. 24, p. 4909, 1999.
- [32] G. Adesso, S. Ragy, and A. R. Lee, “Continuous variable quantum information: Gaussian states and beyond,” *Open Systems & Information Dynamics*, vol. 21, no. 01n02, p. 1440001, 2014.
- [33] T. Plastow and R. Schubert, “Semiclassical methods for investigating open quantum systems and decoherence,” Ph.D. dissertation, University of Bristol, 2020.
- [34] B. Oksendal, *Stochastic differential equations: an introduction with applications*. Springer Science & Business Media, 2013.
- [35] E.-M. Graefe and R. Schubert, “Wave-packet evolution in non-Hermitian quantum systems,” *Physical Review A*, vol. 83, no. 6, p. 060101, 2011.